Localization of the Unruh Effect

Kevin Player[*][†]

June 23, 2025

> The Unruh effect tells us that what we call particles is really just a matter of perspective.

<div align="right">Lee Smolin</div>

Abstract

We present a framework that interpolates between the conventional thermal description of the Unruh effect and a fully localized, non-thermal excitation. In a uniformly accelerating frame, the extended support of Rindler modes across the wedge leads to red- and blue-shifted components, mixing frequencies in a manner that gives rise to the familiar thermal response. To refine this picture, we introduce a partially localized perspective: using modular automorphisms, we map modes between nested Rindler wedges and analyze their localization properties. We further interpolate to compactly approximated wave modes using parabolic cylinder functions, enabling a smooth transition from global to local behavior. While the standard interpretation attributes particle detection to horizon thermality, our construction suggests an alternative mechanism, modeling the observed response as arising from thrust: a localized, directed energy input into the field.

1 Introduction

The Unruh effect[1] reveals that uniformly accelerated observers perceive the Minkowski vacuum as a thermal state, detecting a bath of particles where inertial observers see none. This phenomenon is usually presented by comparing negative-frequency Minkowski modes to positive-frequency Rindler modes, leading to Bogoliubov transformations that mix creation and annihilation operators[2]. The standard explanation relies on the extended nature of Rindler modes, which span the entire wedge and undergo both red-shift and blue-shift along their support.

In this work, we develop a complementary viewpoint by examining how localization affects the thermal character of the field. In Section 2, we review of the Unruh effect, including the relevant mode expansions and Bogoliubov transformations. In Section 3, we apply a classical source construction [3] to inject particles into the field. When targeted at negative-frequency Unruh modes, this setup reproduces the familiar Rindler particle spectrum matching the Bogoliubov analysis.

Section 4 explores partial localization by considering sub-regions of the Rindler wedge related through space-like translations and reflections, transformations that correspond to modular automorphisms in the associated operator algebras. We then use parabolic

---

[*]kplayer@andrew.cmu.edu

[†]kjplaye@gmail.com

cylinder functions to construct a smooth interpolation between eternal Rindler modes and fully localized modes. Finally, in Section 5, we interpret the implications of our construction. These results suggest an alternative interpretation: that the Unruh effect may be understood in terms of localized, non-thermal field excitations that resemble a thrust-like driving force on the field.

2 Preliminaries

We draw notation and standard results from Frodden and Valdés [4]. Let $\hbar = c = 1$. We consider a uniformly accelerating observer in 1+1 dimensional Minkowski spacetime with metric signature $\eta = (-1, +1)$. The extension to 1+3 dimensions does not affect the key physics of the Unruh effect, so we restrict to the (t,x) plane where the boost is occurring. We only consider free scalar fields in this note.

Consider the free scalar massless Lagrangian

$$\mathcal{L}_{free} = -\frac{1}{2}\eta^{\mu\nu}\partial_\mu\phi\partial_\nu\phi. \tag{1}$$

We consider positive frequency modes with dispersion relation $\omega_k = |k| > 0$ as solutions to the resulting Klein-Gordon equation

$$\Box\phi = -\frac{\partial^2\phi}{\partial t^2} + \frac{\partial^2\phi}{\partial x^2} = 0, \tag{2}$$

where $\Box = \eta^{\mu\nu}\partial_\mu\partial_\nu$. We expand ϕ in terms of ladder operators $a_k, a_k^\dagger$

$$\phi(x,t) = \int \mathrm{d}k\, a_k \varphi_k(x,t) + \text{h.c.} \tag{3}$$

where

$$\varphi(x,t) = \frac{1}{\sqrt{4\pi\omega_k}}e^{i(kx - \omega_k t)}. \tag{4}$$

are pure Minkowkski positive frequency waves normalized with respect to the Klein-Gordon inner product over a Cauchy surface Σ (usually $t = 0$)

$$\langle f, g\rangle_{KG} = i\int_\Sigma \mathrm{d}x(f^*\partial_t g - \partial_t f^* g). \tag{5}$$

2.1 Rindler Coordinates

To describe the physics from the point of view of a uniformly accelerating observer, we introduce Rindler coordinates [4, 6] covering a right wedge

$$W = \{(x,t) : x > |t|\} \tag{6}$$

with apex at the origin, pictured[1] in Figure 1; with coordinates

$$t = \frac{1}{a}e^{a\xi}\sinh(a\eta) \tag{7}$$

$$x = \frac{1}{a}e^{a\xi}\cosh(a\eta) \tag{8}$$

The constant acceleration parameter a is introduced explicitly to make the dependence of the Unruh temperature, $T = \frac{a}{2\pi}$, manifest in subsequent expressions. The coordinates (η, ξ) describe the proper time and position in the frame of a uniformly accelerating observer,

Figure 1: Rindler wedge W on the right.

with world-lines of constant ξ corresponding to hyperbolic trajectories in Minkowski space-time.

The massless Klein-Gordon equation in Rindler coordinates is

$$\Box\phi = e^{-2a\xi}(-\partial_\eta^2 + \partial_\xi^2)\phi = 0 \tag{9}$$

The wave equation retains the same structure as the Minkowski case, up to the overall conformal factor $e^{-2a\xi}$. Since this factor does not affect the null structure of the equation, the mode solutions retain the same plane wave form but in the Rindler coordinates

$$r_k(\eta,\xi) = \frac{1}{\sqrt{4\pi\omega_k}}e^{-i(\omega_k\eta - k\xi)} + \text{h.c.} \tag{10}$$

for each wave number k and positive frequency $\omega_k = |k| > 0$. These "Rindler modes" are in terms of η and ξ and are thus confined to the Rindler wedge W. Since Rindler coordinates only cover W (the right wedge), these modes are not defined globally in Minkowski space.

2.2   Unruh Modes

To review how a uniformly accelerated observer perceives the Minkowski vacuum as a thermal bath, we construct the Unruh modes[1], analytic continuations of Rindler modes that are positive-frequency solutions with respect to Minkowski time[2]. From now on let $\omega_k = k > 0$.

We define constants α_k and β_k which satisfy $\alpha_k^2 - \beta_k^2 = 1$

$$\begin{aligned}
\alpha_k &= \frac{e^{\frac{\pi\omega_k}{2a}}}{\sqrt{2\sinh\frac{\pi\omega_k}{a}}} = \sqrt{\frac{1}{1 - e^{-2\pi\omega_k/a}}} \\
\beta_k &= \frac{e^{\frac{-\pi\omega_k}{2a}}}{\sqrt{2\sinh\frac{\pi\omega_k}{a}}} = \sqrt{\frac{1}{e^{2\pi\omega_k/a} - 1}} \quad \text{(thermal form)}
\end{aligned} \tag{11}$$

They show up throughout in mode normalizations[3], inner products, and resulting Bogoloubov transforms. β_k also describes particle creation in terms of $|\beta_k|^2$ which has a thermal character.

Let $\widetilde{W}$ be the left Rindler wedge[4], $x < -|t|$ with Rindler modes $l_{\pm k}$. We analytically continue[5] the Rindler modes r_k, r_{-k}, l_k and l_{-k} into the (t,x) plane, these are the Unruh

---

[1] All diagrams follow the convention of t increasing upward and x increasing to the right.

[2] We mean that the modes contain no negative frequency Minkowski components.

[3] The normalizations come from computing the Klein Gordon inner product on Minkowski space and comparing it to inner products on W and $\widetilde{W}$.

[4] Coordinates on this wedge are $t = -\frac{1}{a}e^{a\delta}\sinh(a\gamma)$, $x = -\frac{1}{a}e^{a\delta}\cosh(a\gamma)$; and $l_{\pm k} = \frac{1}{\sqrt{4\pi\omega_k}}e^{i\omega_k(\gamma\pm\delta)}$.

[5] From the definitions and properties of sinh and cosh, it follows that $a(\pm t + x) = e^{a(\pm\eta + \xi)}$ and then $r_{\pm k} = e^{\pm\frac{i\omega_k}{a}\log a(\mp t + x \pm i\epsilon)}$. Similiar statements hold for the left wedge.

modes

$$\mu_{\pm k}^R = \frac{\alpha_k}{\sqrt{4\pi\omega_k}}(a(\mp t + x \pm i\epsilon))^{\pm\frac{i\omega_k}{a}} \qquad \mu_{\pm k|W}^R \rightarrow \alpha_k r_{\pm k}$$

$$\mu_{\pm k}^L = \frac{\alpha_k}{\sqrt{4\pi\omega_k}}(a(\mp t - x \pm i\epsilon))^{\pm\frac{i\omega_k}{a}} \qquad \mu_{\pm k|\widetilde{W}}^L \rightarrow \alpha_k l_{\pm k} \tag{12}$$

We added an $i\epsilon$ prescription to dictate which branch of the log to take so that the modes are analytic and bounded on the $\Im(t) < 0$ half plane. This makes the modes positive-frequency with respect to t. Another way of writing the Unruh modes is

$$\mu_{\pm k}^R = \alpha_k r_{\pm k} + \beta_k l_{\mp k}^*$$

$$\mu_{\pm k}^L = \alpha_k l_{\pm k} + \beta_k r_{\mp k}^* \tag{13}$$

where the right and left modes ($r_{\pm k}$ and $l_{\pm k}$) are understood to be zero outside of their respective wedges. See Figure 2 for an illustration of the Unruh modes. The magnitude shown jumps across the branch cut and conjugates the phase. Also, note that we have "twice as many" Unruh modes as we have Rindler modes; we double count each r_k with two analytic extensions μ_k^R and μ_{-k}^{L*}, and simliarly for the left modes.

The Unruh modes form an alternative orthonormal basis of solutions to the Klein-Gordon equation, distinct from the plane waves $\varphi_{\pm k}$ see the original source Unruh[1]. The Unruh modes diagonalize (we will see in equation (17)) the Minkowski vacuum in terms of Rindler particle states and thus provide the natural framework for describing the Unruh effect and the thermal response perceived by uniformly accelerated observers.
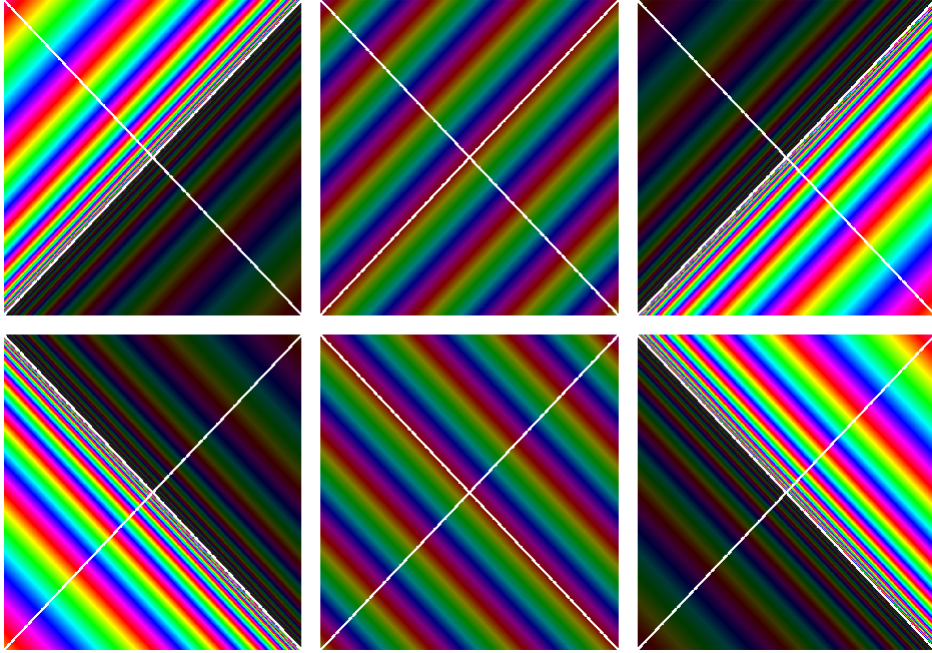

Figure 2: Spacetime diagrams of the $k > 0$ mode functions $\begin{bmatrix} \mu_{-k}^L & \varphi_k & \mu_k^R \\ \mu_k^L & \varphi_{-k} & \mu_{-k}^R \end{bmatrix}$. Color encodes the phase; brightness indicates magnitude. The Unruh modes change magnitude and conjugate phase across the log branch due to the interpretation of $\log(-1\pm i\epsilon)$. The left-moving modes (top) correspond to emission in Minkowski space; the right-moving modes (bottom) to absorption.

2.3   Bogoliubov Transforms

We generalize the wedge W to a translated wedge W_c with apex $(0, c)$

$$W_c = \{(t, x) : x - c > |t|\} \tag{14}$$

and a reflected (left) wedge $\widetilde{W_c}$ with apex $(0, c)$

$$\widetilde{W_c} = \{(t, x) : x - c < -|t|\}. \tag{15}$$

Let the superscripts (0), (c), $(\widetilde{c})$, and (M) represent the W_0, W_c, $\widetilde{W_c}$, and Minkowski frames of reference respectively. Let $(A \to B)$ represent an open set inclusion[6] $A \subseteq B$.

This allows us to directly compute $W_0 \to M$ Bogoliubov coefficients from equation (13) for a change of basis from $a_q^{(M)}$ to c_q^R and c_q^L

$$\phi = \int \mathrm{d}q \ \mu_q^R c_q^R + \mu_q^L c_q^L + \text{h.c.} \tag{16}$$

We find a 4 by 4 block matrix with blocks of the form

$$\begin{bmatrix} a_k^{(0)} \\ a_{-k}^{\widetilde{(0)}\dagger} \end{bmatrix} = \begin{bmatrix} \alpha_k & \beta_k \\ \beta_k & \alpha_k \end{bmatrix} \begin{bmatrix} c_k^R \\ c_{-k}^{L\dagger} \end{bmatrix} \tag{17}$$

and three others, where the $a_{-k}^{\widetilde{(0)}\dagger}$ is a left wedge annihilator. We can summarize the transform in the right wedge W as

$$a_k^{(0)} = \alpha_k c_k^R + \beta_k c_{-k}^{L\dagger} \tag{18}$$

and three other similar relations for $a_{-k}^{(0)}$, $a_k^{(0)\dagger}$, and $a_{-k}^{(0)\dagger}$.

We next compute the more general non-diagonal mixed Bogoliubov transformations.

$$\begin{aligned} (c \to M): \quad a_k^{(c)} &= \int \mathrm{d}q \ \alpha_{kq}^{(c \to M)} a_q^M + \beta_{kq}^{(c \to M)} a_q^{(M)\dagger} \\ (c \to 0): \quad a_k^{(c)} &= \int \mathrm{d}q \ \alpha_{kq}^{(c \to 0)} a_q^{(0)} + \beta_{kq}^{(c \to 0)} a_q^{(0)\dagger} \\ (\widetilde{c} \to 0): \quad a_k^{(\widetilde{c})} &= \int \mathrm{d}q \ \alpha_{kq}^{(\widetilde{c} \to 0)} a_q^{(0)} + \beta_{kq}^{(\widetilde{c} \to 0)} a_q^{(0)\dagger} \end{aligned} \tag{19}$$

We make use of a gamma function for $(c \to M)$. This occurs naturally in the KG dot product as an integral over an exponential phase from φ_k and a $(x - c)$ power from $r_k^{(c)}$ (the Mellin transform of e^{ikx} [8]):

$$\begin{aligned} \alpha_{kq}^{(c \to M)} &= \left\langle \varphi_q, r_k^{(c)} \right\rangle = \frac{1}{2\pi a} \sqrt{\frac{\omega_k}{\omega_q}} \left(\frac{a}{q}\right)^{\frac{i\omega_k}{a}} e^{\frac{\pi\omega_k}{2a}} \Gamma\left(\frac{i\omega_k}{a}\right) \\ \beta_{kq}^{(c \to M)} &= \left\langle \varphi_q^*, r_k^{(c)} \right\rangle = \frac{1}{2\pi a} \sqrt{\frac{\omega_k}{\omega_q}} \left(\frac{a}{q}\right)^{\frac{i\omega_k}{a}} e^{\frac{-\pi\omega_k}{2a}} \Gamma\left(\frac{i\omega_k}{a}\right) \end{aligned} \tag{20}$$

Next we consider products of shifted powers to go after $(c \to 0)$. We make use of a beta function for $(c \to 0)$ which occurs naturally in the KG dot product as an integral over a power of x and of $x - c$, from $r_k^{(0)}$ and $r_k^{(c)}$ respectively. We compute the Bogoliubov coefficients as

$$\begin{aligned} \alpha_{kq}^{(c \to 0)} &= \left\langle r_q^{(0)}, r_k^{(c)} \right\rangle = \frac{1}{2\pi a} \sqrt{\frac{\omega_k}{\omega_q}} (ac)^{\frac{i(\omega_k - \omega_q)}{a}} B\left(\frac{i\omega_k}{a}, \frac{-i(\omega_k - \omega_q)}{a}\right) \\ \beta_{kq}^{(c \to 0)} &= \left\langle r_q^{(0)*}, r_k^{(c)} \right\rangle = \frac{1}{2\pi a} \sqrt{\frac{\omega_k}{\omega_q}} (ac)^{\frac{i(\omega_k + \omega_q)}{a}} B\left(\frac{i\omega_k}{a}, \frac{-i(\omega_k + \omega_q)}{a}\right) \end{aligned} \tag{21}$$

The reflected diamond wedge version also yields a beta function, but with a different form

$$\begin{aligned} \alpha_{kq}^{(\widetilde{c} \to 0)} &= \left\langle r_q^{(0)*}, r_k^{(\widetilde{c})} \right\rangle = \frac{1}{2\pi a} \frac{\sqrt{\omega_k \omega_q}}{\omega_q - \omega_k} (ac)^{\frac{i(\omega_k - \omega_q)}{a}} B\left(\frac{i\omega_k}{a}, -\frac{i\omega_q}{a}\right) \\ \beta_{kq}^{(\widetilde{c} \to 0)} &= \left\langle r_q^{(0)}, r_k^{(\widetilde{c})} \right\rangle = \frac{1}{2\pi a} \frac{\sqrt{\omega_k \omega_q}}{\omega_q + \omega_k} (ac)^{\frac{i(\omega_k + \omega_q)}{a}} B\left(\frac{i\omega_k}{a}, \frac{i\omega_q}{a}\right) \end{aligned} \tag{22}$$

---

[6]In the algebraic formulation of QFT, spacetime regions correspond to operator algebras. Here, we adopt a complementary (though formally contravariant) perspective, whereby shifts in the wedge induce Bogoliubov transformations between operator algebras.

2.4 Modular Automorphisms

We can compare absolute magnitudes for M v.s. W_c and see that they don't depend on c

$$\begin{aligned}
\left|\alpha_{kq}^{(c_1 \to M)}\right|^2 &= \left|\alpha_{kq}^{(c_2 \to M)}\right|^2 \\
\left|\beta_{kq}^{(c_1 \to M)}\right|^2 &= \left|\beta_{kq}^{(c_2 \to M)}\right|^2
\end{aligned} \tag{23}$$

The c independence is expected in this case since Unruh radiation is translation invariant. We next turn to $(c \to 0)$ and also find c independence there

$$\begin{aligned}
\left|\alpha_{kq}^{(c_1 \to 0)}\right| &= \left|\alpha_{kq}^{(c_2 \to 0)}\right| \\
\left|\beta_{kq}^{(c_1 \to 0)}\right| &= \left|\beta_{kq}^{(c_2 \to 0)}\right|
\end{aligned} \tag{24}$$

This invariance is more surprising than in the Minkowski case, as it implies that the expected number of excitations for a mode $r_k^{(c_2)}$ when expressed in the vacuum of W_{c_1},

$$\int \mathrm{d}q \, |\beta_{kq}^{(c_2 \to c_1)}|^2 \tag{25}$$

is invariant[7] under changes in both c_1 and c_2.

More explicitly using the form of the c term in equations (21) and (22) we have a transform matrix of Λ_c from W_0 to W_c

$$\begin{bmatrix} a_k^{(c)} \\ a_{-k}^{(c)} \\ a_k^{(c)\dagger} \\ a_{-k}^{(c)\dagger} \end{bmatrix} = \underbrace{\left[\begin{array}{cc|cc} A_c & 0 & B_c & 0 \\ 0 & -A_c & 0 & -B_c \\ \hline \overline{B_c} & 0 & \overline{A_c} & 0 \\ 0 & -\overline{B_c} & 0 & -\overline{A_c} \end{array} \right]_{k,q}}_{\Lambda_c} \begin{bmatrix} a_q^{(0)} \\ a_{-q}^{(0)} \\ a_q^{(0)\dagger} \\ a_{-q}^{(0)\dagger} \end{bmatrix} \tag{26}$$

where $A_c = \alpha_{kq}^{(c \to 0)} = P_c A_1 P_c^{-1}$ and $B_c = \beta_{kq}^{(c \to 0)} = P_c B_1 P_c$ for a diagonal phase factor matrix

$$P_{c,rs} = \delta(r-s) c^{\frac{i\omega_r}{a}} = e^{\frac{iH}{a} \log c} \tag{27}$$

where H is the Rindler Hamiltonian associated with mode frequency ω_k. We can write Λ_c out compactly out as

$$\Lambda_c = Q_c \Lambda_1 Q_c^{-1} \tag{28}$$

where

$$Q_c = \begin{bmatrix} P_c, & 0 & 0 & 0 \\ 0 & P_c & 0 & 0 \\ 0 & 0 & P_c^{-1} & 0 \\ 0 & 0 & 0 & P_c^{-1} \end{bmatrix} \tag{29}$$

The composition of Bogoliubov transforms, $\Lambda_{nc} = \Lambda_c^n$, yields

$$\begin{aligned}
Q_{nc} \Lambda_1 Q_{nc}^{-1} &= \Lambda_{nc} \\
&= (Q_c \Lambda_c Q_c) \left(Q_c^{-1} \Lambda_c Q_c \right) \cdots (Q_c \Lambda_c Q_c) \\
&= Q_c \Lambda_c^n Q_c^{-1}
\end{aligned} \tag{30}$$

so that

$$\begin{aligned}
\Lambda_c^n &= Q_c^{-1} Q_{nc} \Lambda_1 Q_{nc}^{-1} Q_c \\
&= Q_n \Lambda_1 Q_n^{-1}
\end{aligned} \tag{31}$$

---

[7]Similar statements are true for reflected (diamond) wedges.

and more generally we have a one parameter unitary group under the modular parameter $x = \log c$, with generator H/a given by

$$\left\{ \Lambda_1^x = Q_x \Lambda_1 Q_x^{-1} : x \in \mathbb{R} \right\}. \tag{32}$$

So these Bogoliubov transformations between shifted wedges form a one-parameter group under translations of the apex, exhibiting a symmetry that parallels modular automorphism flow in algebraic QFT [9]. In contrast to traditional treatments emphasizing Lorentz boosts within a fixed wedge, this formulation reveals modular structure via spatial translations.

Consider a sequence

$$W_{c_n} \subseteq \cdots \subseteq W_{c_i} \subseteq \cdots \subseteq W_{c_j} \subseteq W_{c_2} \subseteq W_{c_1} \tag{33}$$

The result is that each inclusion $W_{c_i} \subseteq W_{c_j}$ yields the same "amount" and "type" of particle production, with fixed squared Bogoliubov magnitude $|\beta_{kq}|^2$, implying that the expected number of particles remains constant across all nested wedge pairs, independent of the actual values of c_i or c_j.

3 Driving Sources

We now turn to a foundational question: **"What, physically, is accelerating the observer?"** Up to this point, acceleration has been introduced as a geometric feature, a coordinate choice, without reference to any underlying dynamical mechanism. Moreover, we have left unspecified both the observer's precise location within the Rindler wedge and the spatial origin of the detected excitations. These omissions reflect an effective coarse-graining over the details of the observer and their interaction with the field, a feature that contributes to the apparent thermality observed in the Unruh effect.

A natural physical interpretation is that a *driving source* must exist, both as the cause of the observer's acceleration, and as a localized field source coupled to the quantum field. In this view, acceleration is not merely a kinematic artifact or coordinate reparameterization, but the result of active, localized interactions along the observer's worldline. These interactions are responsible for the observer's motion.

Figure 3 illustrates the situation with a particle composed of Rindler modes. The modes r_k are left-moving, propagating toward the future horizon and interpreted as **emission**; the r_{-k} modes are right-moving, originating from the past horizon and interpreted as **absorption**. These Rindler modes are constructed as superpositions of restricted Minkowski modes $\varphi_{q|_W}$, effectively smeared across a range of frequencies. This frequency mixing is evident in Figure 2, where the modes blue-shift infinitely near the horizons and red-shift infinitely at spatial infinity, due to the geometry of the wedge.

The mathematical underpinning of this effect is encoded in the Bogoliubov coefficients $\alpha_{kq}^{(c \to M)}$ and $\beta_{kq}^{(c \to M)}$, which express the Rindler modes in terms of their Klein-Gordon inner products with Minkowski positive- and negative-frequency modes, φ_q and φ_q^*, respectively[8]. This delocalization in frequency space, rooted in the extended support of the Rindler modes and tied to the observer's causal horizon, plays a central role in producing the thermal spectrum characteristic of the Unruh effect.

To address this, we now introduce the driving source, a standard construction [3] [10], and a physical mechanism that excites the field and, directly, accounts for the observer's acceleration. This reframes the interpretation: rather than a spontaneous thermal response associated with entanglement across a causal horizon, the observed acceleration emerges from a dynamically injected coherent excitation, rather than from vacuum squeezing across a horizon. An illustration of this setup is shown in Figure 4. From this

---

[8] φ_q is restricted to W since r_k is supported on W.

Figure 3: A Rindler mode's frequency is smeared out in Minkowski space, blue-shifted near the horizon. We diagram a particle as if it were striking a mirror at the rear of a rocket, where its reflection emerges as a combination of emission and absorption processes in the Rindler frame.

perspective, the apparent thermality arises not from intrinsic properties of the vacuum, but from an effective ignorance of the source's detailed structure and dynamics. In this view, the Unruh effect is not a passive revelation of hidden particles in the vacuum, but a measurable consequence of *thrust*.

To model this process, we aim to match the effect of a field-theoretic creation operator by introducing a classical source term $J(x)$ into the Lagrangian, applied at a finite time interval.

$$\mathcal{L}_{sourced} = \mathcal{L}_{free} + J\phi \tag{34}$$

The source couples linearly to the field and excites a specific mode, thereby preparing a coherent state whose phase and amplitude are determined by the source profile. In order to replicate the targeted excitation, $J(x)$ must be engineered so that its inner product with the mode functions matches the effect of the creation operator acting on the vacuum.
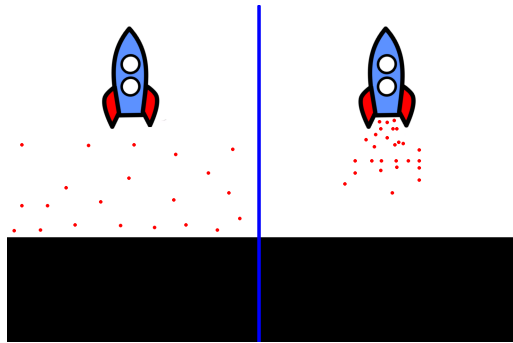

Figure 4: Conceptual illustration of thermal v.s. localized acceleration.

The field can be expanded as in equation (16), and the β_k-term in equation (18) is responsible for the thermal particle content of the Minkowski vacuum as seen by (right wedge) Rindler observers. For clarity, we first present the construction for a single μ_{-k}^{L*}-mode. Because the Rindler modes, form a complete orthonormal set under the Klein-Gordon inner product on the right wedge, this construction extends linearly and independently to the full family of modes. We encode the effect of a creation operator $c_{-k}^{L\dagger}$

8

using

$$c_{-k}^{L\dagger} = \langle \phi, \mu_{-k}^{L*} \rangle_{KG} = \int \mathrm{d}x \; \mu_{-k}^{L*}(x)\phi(x) \tag{35}$$

and the orthogonality of the mode functions in the Klein-Gordon inner product.

The modes are constructed to have purely negative frequency with respect to right Rindler time η. This ensures that the source couples to physical creation operators and injects particles into the field in a well-defined way. The resulting excitation respects the correct Minkowski vacuum structure while encoding the full Rindler response.

In the generating functional formalism, setting $J = -\beta_k u_k^{L*}$ the functional derivative $\frac{\delta}{\delta J}Z[J]|_{J=0}$ inserts ϕ into time-ordered correlators. Smearing this field insertion against $\mu_{-k}^{L*}(x)$ thus projects onto $c_{-k}^{L\dagger}$ and we have

$$\begin{aligned} a_k^{(0)J} &= \alpha_k c_k^R + \beta_k c_{-k}^{L\dagger} - \beta_k c_{-k}^{L\dagger} \\ &= \alpha_k c_k^R \end{aligned} \tag{36}$$

The source is also correlated with the left wedge where we pick up a β_k factor times a left annihilator (see equation (17)), but we don't see that in the right wedge. This is a source correlation which is usually thought of as an entangled vacuum. We are essentially saying that particles found in the right wedge "come from" the left wedge or at least some casual past.

In Rindler coordinates, the presence of this source term prepares a modified field state in which the Rindler mode occupation deviates from the thermal distribution that characterizes the Minkowski vacuum. Rather than simply injecting energy into the field, the source introduces a coherent excitation that interferes with the mode structure induced by the Bogoliubov β-terms. Effectively, the source cancels the thermal contribution of the Bogoliubov β-term for the targeted mode, allowing construction of a modified field state in which a Rindler detector registers no particles at that frequency.

$$\langle J| b_k^\dagger b_k |J\rangle = \langle 0_M| b_k^J b_k^J |0_M\rangle = 0 \tag{37}$$

Thus, while the spectrum observed by accelerated observers matches that predicted by the thermal Bogoliubov analysis, it is here derived from a definite, localized dynamical cause, not an entangled vacuum. In this perspective, the chain of inclusions in equation (33) is realized as a causal sequence, not of vacuum correlations, but of physically sourced particle injections propagating between shifted wedges. The c-independence of the modular automorphism, often taken as a structural symmetry, is then reinterpreted as a manifestation of transitivity among these injections: particle content transmitted from W_{c_i} to W_{c_j} is invariant under intermediate steps.

This construction reproduces the Rindler particle spectrum predicted by the Bogoliubov transformation, but with a key difference: the observed response now results from a well-defined dynamical process rather than a statistical average over inaccessible degrees of freedom. Provided the excited modes form a Klein-Gordon orthonormal basis, such as the Unruh modes, this equivalence holds when using causal (retarded) or time-ordered (Feynman) Green's functions. These propagators allow linear superpositions of negative-frequency components to act as physically realizable particle injections.

4 Localization

4.1 Localization via Translated Wedge Inclusion

Consider the two nested Rindler wedges $W_c \subseteq W_0$ shown in Figure 5. Let r_q denote a Rindler mode[9] associated with W_0, analytically continued to the entire Minkowski space.

---

[9]From here on we often interchange Rindler and Unruh modes since we are only concerned with the restriction to the right wedge or subsets.

The gray-scale region indicates the full support of r_q, while the rainbow-colored segment shows its restriction to the sub-wedge W_c.
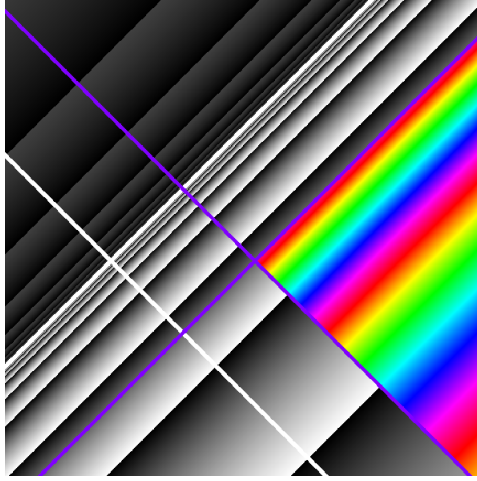

Figure 5: A Wedge W_c (blue) inside of the wedge W_0 (white). Rindler mode r_q of W_0 (gray-scale) restricted to W_c (rainbow).

By considering the restriction of r_q to W_c, we have partially localized the observer and the mode. The restriction effectively cuts off the high-frequency content of r_q near the future horizon[10] of W_0. The resulting mode still spans the full spatial extent of W_c, but it is now insulated from the highly oscillatory behavior near the horizons of W_0. The localization is not complete however, the observer can still be anywhere within the wedge W_c, and the corresponding modes r_k still exhibit thermal characteristics because of low-frequency oscillations extending throughout the wedge.

To further study the situation, consider the modulus squared inner product $\left|\left\langle r_q^{(0)}, r_k^{(c)} \right\rangle\right|^2$, also known as the Bogoliubov $\left|\alpha_{kq}^{(c\to 0)}\right|^2$, from equation (21). We fix q and use $|\Gamma(ib)|^2 = \frac{\pi}{b\sinh \pi b}$ to obtain

$$\left|\left\langle r_q^{(0)}, r_k^{(c)} \right\rangle\right|^2 = \frac{\sinh \frac{\pi\omega_q}{a}}{4\pi a(\omega_q - \omega_k)\sinh \pi \frac{\omega_q - \omega_k}{a} \sinh \frac{\pi\omega_k}{a}} \tag{38}$$

as a function of ω_k. The function exhibits a second-order pole at $\omega_k = \omega_q$, resulting in a sharply peaked feature, see Figure 6. Although the sinh terms encode aspects of the familiar thermal distribution, especially broadening near $\omega_k = 0$, the existence of the peak itself at $\omega_k = \omega_q$ originates from the geometric restriction, not from a detector's passive response to the vacuum, but as the active spectral footprint of a localized source.

4.2 Diamond Localization via Reflected Wedge Intersection

Further localization is achieved by intersecting W_c with a reflected wedge $\widetilde{W}_{2c}$. This defines a more tightly localized diamond-shaped region, as shown in Figure 7. The mode r_q is now restricted to the intersection $W_c \cap \widetilde{W}_{2c}$, which eliminates much of the infrared behavior previously associated with the unrestricted wedge.

The Klein Gordon inner product at $t = 0$ now takes the form of an incomplete version of the beta function from equation (21), corresponding to an integral[11] evaluated from c to $2c$ rather than extending to infinity. This inner product does not however correspond

---

[10]Similarly, r_{-q} experiences suppression near the past horizon.

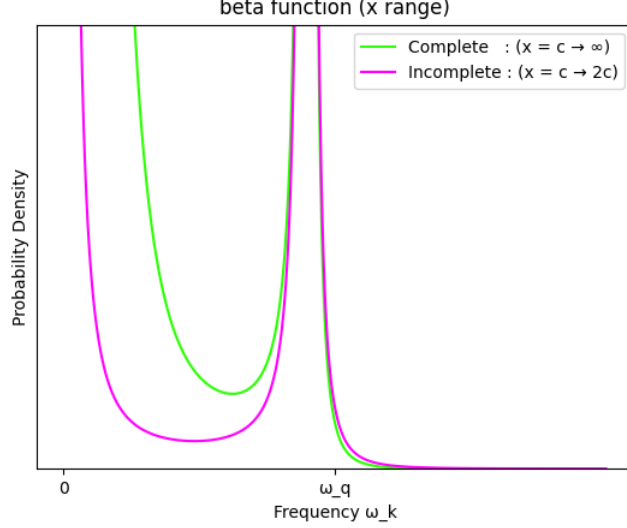[11]We could also use the other form of the beta function in equation (22) to compute the same inner product.

Figure 6: The Rindler modes r_k of W_c show a peaked spectral overlap with r_q at $\omega_k = \omega_q$. The incomplete beta function picks out the spectral peak suppressing the peak at zero.

to a mode expansion of the field, since the analytic continuation of the diamond would be to all of W_c, or all of $\widetilde{W}_{2c}$, in which case the mode would no longer be localized to the diamond. So it is no longer invariant to integrate along a Cauchy surface for the inner product; this construction does not define a complete orthonormal set, and cannot be used to build a full basis of field modes.

This motivates a shift in perspective: rather than interpreting r_q as part of a global mode expansion, we regard it as a compactly supported, non-invariant test function, i.e., a driving source localized to the diamond region, consistent with the source framework introduced in Section 3. We turn on r_q exactly for a fixed period of $x - t$ (or $x + t$ for r_{-q}). The resulting spectral response in the diamond, computed from this truncated integral, is shown[12] in Figure 6.

The plot reveals that the main spectral peak at $\omega_k = \omega_q$ persists, while the thermal contribution near $\omega = 0$ is significantly attenuated.

4.3 Thermal to Localized Interpolation

To further probe how global thermal structure transitions into a localized excitation profile, we consider the behavior of Rindler-to-Minkowski Bogoliubov coefficients when weighted by a Gaussian envelope. This allows us to interpolate between de-localized (thermal) and localized (spectrally peaked) behavior. We use parabolic cylinder functions [11, 12] which are the analytic continuation of

$$D_\nu(-z) = \frac{e^{-\frac{1}{4}z^2}}{\Gamma(-\nu)} \int_0^\infty \mathrm{d}s \; e^{zs} s^{-\nu-1} e^{-\frac{1}{2}s^2}, \Re\nu < 0, \tag{39}$$

where we use $-z$ instead of the usual z so that future equations become simpler.

Without loss of generality, let $N_{\mu,\sigma} = e^{-\frac{1}{2}\frac{(x-t-\mu)^2}{\sigma^2}}$ be a (left-moving) Gaussian kernel with fixed μ. We will multiply φ_q^* by $N_{\mu,\sigma}$, but we could just as easily multiply r_k by $N_{\mu,\sigma}$ for the same effect. A key aspect of this construction is that the resulting Minkowski modes

---

[12]The green (complete) beta function curve is actually independent of the choice of translation c, it is the same curve for any sub-wedge space-like inclusion (see Modular Automorphism Section 2.4). In contrast, the incomplete beta function curve (magenta) does depend on the endpoint ($2c$ is shown).
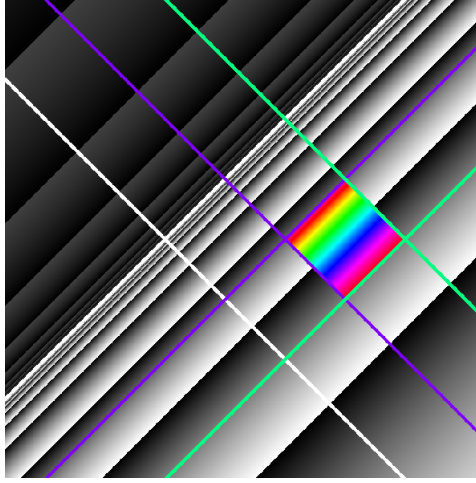
Figure 7: The same situation as in Figure 5 but we further intersect with a reflected (left) wedge $\widetilde{W}_{2c}$ (green). Rindler mode r_q of W_0 (gray-scale) restricted to $W_c \cap \widetilde{W}_{2c}$ (rainbow).

are treated as driving sources rather than elements of an orthonormal mode expansion. Since we are not working within an orthonormal mode expansion, the normalization of $N_{\mu,\sigma}$ is left implicit. For clarity, since this setup may be non-standard, we carry out the calculations explicitly in this section. We will examine the $N_{\mu,\sigma}$ modification of $\beta_{kq}^{(c \to M)}$ in equation (20)

$$
\begin{aligned}
\langle \varphi_q^* N_{\mu,\sigma}, r_k \rangle &= \frac{1}{4\pi \sqrt{\omega_q \omega_k}} 2i \int_{\Sigma_W} e^{-i(\omega_q t - qx)} e^{-\frac{1}{2}\frac{(x-t-\mu)^2}{\sigma^2}} \partial_t (a(x-t))^{\frac{i\omega_k}{a}} \\
&= \frac{1}{2\pi} \sqrt{\frac{\omega_k}{\omega_q}} a^{\frac{i\omega_k}{a}-1} \int_0^\infty \mathrm{d}x \; e^{-\frac{1}{2}\frac{(x-\mu)^2}{\sigma^2}+iqx} x^{\frac{i\omega_k}{a}-1} \\
&= \frac{1}{2\pi} \sqrt{\frac{\omega_k}{\omega_q}} a^{\frac{i\omega_k}{a}-1} \int_0^\infty \mathrm{d}x \; e^{\left(-\frac{1}{2\sigma^2}\right)x^2 + \left(\frac{\mu}{\sigma^2}+iq\right)x + \left(-\frac{\mu^2}{2\sigma^2}\right)} x^{\frac{i\omega_k}{a}-1} \\
&= \frac{1}{2\pi a} \sqrt{\frac{\omega_k}{\omega_q}} e^{-\frac{\mu^2}{2\sigma^2}} \sigma^{\frac{i\omega_k}{a}} a^{\frac{i\omega_k}{a}} \int_0^\infty \mathrm{d}s \; e^{\left(\frac{\mu}{\sigma}+iq\sigma\right)s} s^{\frac{i\omega_k}{a}-1} e^{-\frac{1}{2}s^2} \\
&= \frac{1}{2\pi a} \sqrt{\frac{\omega_k}{\omega_q}} e^{-\frac{\mu^2}{2\sigma^2}} (\sigma a)^{\frac{i\omega_k}{a}} e^{\frac{1}{4}\left(iq\sigma+\frac{\mu}{\sigma}\right)^2} \Gamma\left(\frac{i\omega_k}{a}\right) D_{-\frac{i\omega_k}{a}}\left(-iq\sigma-\frac{\mu}{\sigma}\right) \\
&= \frac{1}{2\pi a} \sqrt{\frac{\omega_k}{\omega_q}} e^{-\frac{\mu^2}{2\sigma^2}} (\sigma a)^{\frac{i\omega_k}{a}} e^{\frac{1}{4}z^2} \Gamma(-\nu) D_\nu(-z)
\end{aligned}
\tag{40}
$$

where Σ_W is the Cauchy surface $\eta = 0$ on the Rindler wedge W, $x = \sigma s$, $z = iq\sigma + \frac{\mu}{\sigma}$, and $\nu = -\frac{i\omega_k}{a}$. And then

$$
\left|\langle \varphi_q^* N_{\mu,\sigma}, r_k \rangle\right|^2 = \frac{1}{2\pi a \omega_q} \frac{\omega_k}{2\pi a} e^{-\frac{\mu^2}{\sigma^2}} \left| e^{\frac{1}{2}z^2} \right| |\Gamma(-\nu)|^2 |D_\nu(-z)|^2
\tag{41}
$$

From [12] we have

$$
D_\nu(-z) = e^{-i\pi\nu} z^\nu e^{-\frac{1}{4}z^2} \{1 + O(|z|^{-2})\} + \frac{(2\pi)^{\frac{1}{2}}}{\Gamma(-\nu)} z^{-\nu-1} e^{\frac{1}{4}z^2} \{1 + O(|z|^{-2})\}
\tag{42}
$$

when $-\frac{1}{4}\pi + \epsilon \le \arg z \le \frac{3}{4}\pi - \epsilon$.

The two asymptotic regimes correspond to physically distinct interpretations: The second $e^{\frac{1}{4}z^2}$ term dominates for $z \to \infty$ as $\sigma \to 0$ and the first $e^{-\frac{1}{4}z^2}$ term dominates for
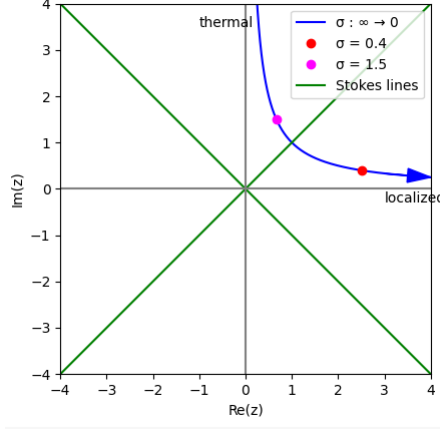
Figure 8: Trajectory of $z = iq\sigma + \frac{\mu}{\sigma}$ as σ interpolates between thermal and localized regimes. For σ starting at ∞, the trajectory starts at the positive infinite imaginary axis, aligning with the dominant thermal component of the excitation. As $\sigma \to 0$, the system crosses a Stokes line and transitions into a sharply localized, source-driven configuration, where thermal character disappears. See also corresponding Figure 9.

$z \to i\infty$ as $\sigma \to \infty$. This is a Stokes phenomenon[13] which flips over as we cross the Stokes line at $\arg z = \frac{\pi}{4}$. The situation is pictured in Figure 8.

We next combine equations (41) and (42). First for the thermal part that comes from the $e^{-\frac{1}{4}z^2}$ term where $\sigma \to \infty$ we have

$$
\begin{aligned}
2\pi a \omega_q \left| \langle \varphi_q^* N, r_k \rangle \right|^2 &= \frac{\omega_k}{2\pi a} e^{-\frac{\mu^2}{\sigma^2}} \left| e^{-i\pi\nu} z^\nu \Gamma\left(\frac{i\omega_k}{a}\right) \right|^2 \\
&= \frac{\omega_k}{2\pi a} e^{-\frac{\mu^2}{\sigma^2}} e^{\frac{-2\pi\omega_k}{a}} \left| e^{\frac{-2i\omega_k}{a}\log\left(\frac{\mu}{\sigma}+iq\sigma\right)} \right|^2 \frac{\pi}{\frac{\omega_k}{a}\sinh\frac{\pi\omega_k}{a}} \\
&\to e^{\frac{-2\pi\omega_k}{a}} \left| e^{\frac{-2i\omega_k}{a}\log i} \right|^2 \frac{1}{2\sinh\frac{\pi\omega_k}{a}} \\
&= e^{\frac{-2\pi\omega_k}{a}} e^{\frac{\pi\omega_k}{a}} \frac{1}{\left(e^{\frac{\pi\omega_k}{a}} - e^{\frac{-\pi\omega_k}{a}}\right)} \\
&= \frac{1}{e^{\frac{2\pi\omega_k}{a}} - 1}
\end{aligned}
\tag{43}
$$

which we expect by construction. For the localized part that comes from the $e^{\frac{1}{4}z^2}$ term where $\sigma \to 0$ we have

$$
\begin{aligned}
2\pi a \omega_q \left| \langle \varphi_q^* N, r_k \rangle \right|^2 &= \frac{\omega_k}{a} e^{-\frac{\mu^2}{\sigma^2}} \left| e^{z^2} z^{2(-\nu-1)} \right| \\
&= \frac{\omega_k}{a} e^{-\frac{\mu^2}{\sigma^2}} \left| e^{\left(iq\sigma+\frac{\mu}{\sigma}\right)^2} e^{2\left(\frac{i\omega_k}{a}-1\right)\log\left(iq\sigma+\frac{\mu}{\sigma}\right)} \right| \\
&\to \frac{\omega_k}{a} e^{\frac{-2\epsilon\omega_k}{a}} f(\sigma, \mu)
\end{aligned}
\tag{44}
$$

where the thermal pole at zero has disappeared. While the precise asymptotic form is not critical, we can control the ultraviolet behavior by taking z to $(1+i\epsilon)\infty$ which remains

---

[13]See [13] for a similar approach where the Stokes phenomenon is applied to particle production in simple expanding backgrounds, preheating after R^2 inflation, and a transition model with smoothly changing mass.
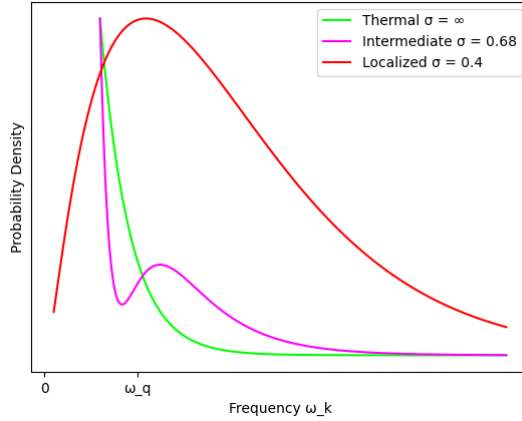
Figure 9: $\left|\left\langle \varphi_q^* N, r_k \right\rangle\right|^2$ for various values of σ (probability density is scaled for comparison). $\omega_q = 1$, $q = 1$, $a = 1$, $\mu = 1$. See also corresponding Figure 8.

within in the localized Stokes region. This introduces a regulating factor of the form $e^{-2\epsilon\omega_k/a}$, which suppresses high-frequency contributions.

We should stop short of σ actually reaching zero, since that is a localization to an extreme, where $N_{\mu,\sigma}$ shrinks to a bump with infinitesimal width; This is not a delta function, it is a vanishing source. We focus on the small-but-nonzero σ regime where the thermal character has already disappeared. See Figure 9 for representative plots across varying values of σ.

5   Conclusion

This work examined the Unruh phenomenon from a localized perspective, emphasizing its manifestation as a physically driven effect rather than a purely thermal one. By restricting Rindler modes to translated and reflected wedges, and their intersections, we showed that the apparent thermal behavior can be partially eliminated. As these modes become localized, the traditional detector response, typically interpreted as a thermal signature of entanglement across a causal horizon, is here reinterpreted as the spectral imprint of a localized, dynamically sourced excitation. We then showed that the mixed Bogoliubov inner product between Minkowski and Rindler modes provides a smooth interpolation from global thermality to a localized spectral structure, with parabolic cylinder functions encoding this transition in analytic form.

Our approach complements the traditional detector-based interpretation by highlighting the role of the physical agent causing acceleration as an active source of field excitations. This perspective does not contradict the well-known thermality arising from entanglement but offers a localized, dynamical viewpoint that may better capture realistic scenarios.

While our analysis is grounded in flat spacetime, the equivalence principle offers a natural pathway for extending this framework to curved geometries. In particular, future work could explore applications to Hawking radiation by modeling localized excitations near black hole horizons. Figure 10 offers a schematic illustration of this idea, emphasizing a shift from thermal emission to localized, physically sourced excitations in the near-horizon region.
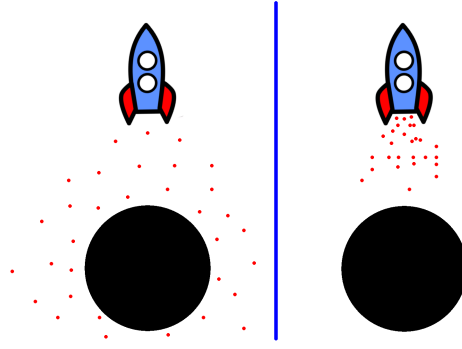
Figure 10: Conceptual illustration contrasting global Hawking radiation (left) with a localized, source-driven excitation near a black hole (right).

6   Acknowledgments

References

[1] W. G. Unruh, "Notes on black-hole evaporation," *Physical Review D*, vol. 14, no. 4, p. 870, 1976.

[2] L. C. Crispino, A. Higuchi, and G. E. Matsas, "The unruh effect and its applications," *Reviews of Modern Physics*, vol. 80, no. 3, pp. 787–838, 2008.

[3] J. Schwinger, "Particles and sources," *Physical Review*, vol. 152, p. 1219â€"1226, Dec. 1966.

[4] E. Frodden and N. Valdes, "Unruh effect: Introductory notes to quantum effects for accelerated observers," *International Journal of Modern Physics A*, vol. 33, no. 27, p. 1830026, 2018.

[5] T. Jacobson, "Introduction to quantum fields in curved spacetime and the hawking effect," in *Lectures on quantum gravity*, pp. 39–89, Springer, 2005.

[6] W. Rindler, "Kruskal space and the uniformly accelerated frame," *Am. J. Phys*, vol. 34, no. 12, pp. 1174–1178, 1966.

[7] R. Haag and D. Kastler, "An algebraic approach to quantum field theory," *Journal of Mathematical Physics*, vol. 5, no. 7, pp. 848–861, 1964.

[8] R. Bracewell and P. B. Kahn, "The fourier transform and its applications," *American Journal of Physics*, vol. 34, no. 8, pp. 712–712, 1966.

[9] H. J. Borchers, "On revolutionizing quantum field theory with tomita's modular theory," *Journal of mathematical Physics*, vol. 41, no. 6, pp. 3604–3673, 2000.

[10] L. H. Ryder, *Quantum field theory*. Cambridge university press, 1996.

[11] M. Abramowitz and I. A. Stegun, eds., *Handbook of Mathematical Functions with Formulas, Graphs, and Mathematical Tables*, vol. 55 of *Applied Mathematics Series*. Washington, D.C.: U.S. Government Printing Office, 1964. Reprinted 1983. See Chapter 19.

[12] F. W. J. Olver, "Uniform asymptotic expansions for weber parabolic cylinder functions of large orders," *Journal of Research of the National Bureau of Standards. Section B, Mathematical Sciences*, vol. 63B, pp. 131–169, 1959.

[13] S. Hashiba and Y. Yamada, "Stokes phenomenon and gravitational particle production—how to evaluate it in practice," *Journal of Cosmology and Astroparticle Physics*, vol. 2021, no. 05, p. 022, 2021.

[14] N. Beisert, "Quantum field theory i," *ETH Zurich, HS12*, 2012.